# Impact of rice bran wax purity and oleogelation conditions on the structural stability of sunflower oil-based oleogels

*Danilo Candela[1], Henriette Brykczynski[2], Cecilia Fiore[1], Eckhard Flöter[2], Elena Simone[3]**

*1 Department of Applied Science and Technology (DISAT), Politecnico di Torino, Torino (Italy)*

*2 Department of Food Process Engineering, Technische Universität Berlin, Berlin (Germany)*

Corresponding author: Prof. Elena Simone (elena.simone@polito.it)

**Keywords:** rice bran wax, oleogelation process, fat replacement, oleogels.

## Abstract

The growing demand for healthier ingredients has driven research toward innovative systems, such as oleogels, which can provide nutritional benefits without compromising food texture and mouthfeel. Among various structuring agents, rice bran wax (RBX) is a promising candidate for creating three-dimensional networks in liquid vegetable oils. However, the functional success of these systems is heavily dependent on wax purity and processing conditions. This study investigates the impact of RBX purity and oleogelation conditions on the structural stability of sunflower oil-based oleogels. A purified RBX (obtained via an optimised isolation protocol) was compared with two commercial alternatives to evaluate the possible influence of interfering compounds on microstructural assembly. Results show that the reduced quantity of impurities in the laboratory-purified RBX allowed for a more cohesive crystalline matrix, yielding enhanced stability even at low concentration (1 %wt) under static gelation conditions. Furthermore, the application of mechanical stirring during the oleogelation phase was found to hinder the development of a continuous solid network, promoting the formation of aggregates that led to significant oil leakage during storage. These findings demonstrate that high-performance oleogels can be achieved by optimizing both wax isolation protocols and environmental

conditions during oleogelation. This research supports the potential for incorporating high-purity RBX oleogels into complex food matrices as a sustainable alternative to saturated fats, contributing to the development of improved lipid-based food products.

## 1. Introduction

In recent years, increasing attention has been paid to what people eat and how diet might affect our health and the environment [1], [2]. Over the last few decades, in fact, significant correlations have been observed in developed nations between non-optimal dietary patterns and the rising incidence of chronic diseases, most notably cardiovascular and oncological pathologies [3], [4]. The emergence of these pathologies is frequently attributed to the high consumption of ultra-processed foods characterised by elevated saturated fat content; such dietary profiles result in a caloric surplus, which might be a primary driver for these conditions [4], [5], [6], [7]. To mitigate these concerns, novel classes of colloidal lipid-based systems have been engineered and designed to optimize nutritional profiles without compromising functional properties. Among these systems, oleogels represent an extensively investigated class due to their diverse functional applications and the vast landscape of potential formulations involving distinct lipid phases and gelling agents [8], [9], [10]. Typically, these structuring agents are blended and incorporated into the liquid oil phase, favouring the development of a three-dimensional network that provides structural integrity to the starting liquid oil [8], [11]. Among the most extensively studied oleogelators, two main classes are generally distinguished: low-molecular (LMWOs) and high-molecular (HMWOs) weight oleogelators [8], [9]. The former category comprises crystalline particles, such as natural waxes, fatty acids, and mono-, di-, or triglycerides, whereas the latter consists of polymers like carbohydrates and proteins. Research has predominantly focused on LMWOs, as their direct solubility in the lipid phase allows for the formation of stable oleogels even at minimal concentrations [12], [13], [14].

Natural waxes are extensively employed oleogelators because they are frequently obtained as agricultural by-products [15], [16], [17]. Integrating these materials back into the production chain enhances environmental sustainability and aligns with circular economy principles [18], [19]. Several types of waxes are used in the preparation of oleogels. The most common ones include beeswax, carnauba wax, candelilla wax, sunflower wax, and rice bran wax (RBX) [8], [20], [21], [22]. While beeswax comes from an animal source (which generally raises ethical concerns about the exploitation of bees [23]), the other types come from plant sources, making them more sustainable and widely accepted alternatives. From a chemical perspective, waxes are heterogeneous substances primarily characterised by long-chain esters derived from the esterification of long-chain fatty acids and alcohols [8], [24], [25]. While wax esters constitute the majority of wax composition, these materials also incorporate a diverse range of minor constituents, including n-alkanes, sterol esters, and pentacyclic triterpenoid derivatives [8]. Such chemical heterogeneity is reflected in their thermal properties, with melting ranges varying from 30°C to 90°C. This highlights the importance of the extraction and purification processes employed, to refine the wax and tailor its properties for specific applications [26].

The combination of thermal and structural features, arising from the specific chemical composition of the wax oleogelator, has a significant impact on the properties of the resulting oleogel [27], [28]. As an example, waxes containing high amounts of wax esters (as is the case of sunflower wax) deliver large, needle-shaped crystals during the oleogelation process, which are highly effective at trapping the liquid phase [20], [29]. The final result is a firm gel that remains stable even at high temperatures and shows better resistance when subjected to mechanical stresses compared to waxes with low content of esters.

RBX represents an ideal case study to investigate these structure-function relationships. Rice bran is an abundant agricultural secondary product coming from the rice milling process. To valorise this residue, rice bran oil can be extracted and commercialised after been refined. RBX is obtained during

the dewaxing step of this refining process, and it is mainly composed of wax esters, but also of some other components as fatty acids, and fatty alcohols. The use of RBX as an oil-gelling agent has been reported in different studies involving several types of vegetable oils [30], [31], [32], [33], [34]. In most cases, RBX has proven to be a compound capable of forming stable crystalline networks at low concentrations. In the work of Wijarnprecha et al., 2018, RBX (ranging from 0.5 %wt and 25 %wt) was blended with rice bran oil and it was found that the 0.5 %wt concentration can produce a stable structure when stored at temperature below 15°C [35]. When prepared with higher RBX's concentrations, the structural, mechanical, and thermal properties of the relative oleogels were found to improve as a function of the network of the interlinked needles crystals formed. A similar behaviour was found also by N. Wang et al., 2021, who observed that, when structuring rice bran oil, a minimum concentration of 7 %wt of RBX was necessary to obtain an oleogel at 20 °C [31]. This significant discrepancy in the minimum gelling concentrations reported (0.5 %wt [35] and 7 %wt [31]) can be attributed to some variations in the purity and laboratory-scale isolation methods of the employed waxes. It is possible that the specific extraction protocol used in the work of N. Wang et al., 2021 led to a lower degree of purity compared to commercial standards. Such impurities can hinder the formation of the crystalline network, requiring a higher wax content to achieve a stable oleogel. Another inconsistent result was reported by Doan et al., 2015 [22]. They observed a minimum RBX concentration of 5 %wt in rice bran oil and justified this phenomenon by pointing out a weaker interaction between the wax and RBO. This weak interaction limits the formation of a tight crystal network, causing the RBW to crystallize into large dendritic structures rather than the highly efficient, needle-like or fibrous networks formed in other vegetable oils such as olive and salad oil. The effect of the composition of the wax used on the properties of the resulting oleogels has been extensively studied by Wettlaufer et al., 2021 [36]. In their work, wax esters are highlighted as the primary drivers of oleogelation due to their linear structure, which promotes rapid gel-sol transitions and low undercooling. Consequently, waxes with high ester content, such as Sunflower Wax and RBX, exhibit enhanced structuring efficiency. Nonetheless, despite their similar wax esters content, sunflower wax

presents a narrower esters distribution, promoting the formation of highly interconnected needle-like crystals resulting in more stable oleogels compared to RBX. Conversely, the presence of high proportions of non-ester components significantly impairs gel performance. For instance, high concentrations of free fatty alcohols (e.g. in carnauba wax [30]) or free fatty acids and hydrocarbons (e.g. in beeswax [37]) induce complex, multi-peak thermal transitions and severe undercooling, ultimately disadvantaging the formation of a cohesive and stable crystalline network.

Effective isolation of RBX requires protocols that prioritize both purity and recovery. Refined extraction steps are necessary to prevent the carryover of contaminants, which, as previously noted, can significantly affect the wax's performance in oleogel systems. In this regard, our previous work [38] proposed five different strategies for isolating RBX from rice bran butter. Although all five processes studied resulted in the isolation of highly pure waxes, only one strategy (referred to in the paper as "Process #2") achieved the best results in terms of extraction yield and purity. The resulting material was characterised in terms of its thermal and structural properties, while the sustainability of the extraction process was evaluated using Life Cycle Assessment (LCA) [38]. Nevertheless, the characterisation of the chemical composition of the obtained wax was not performed and its potential use as an oil-gelling agent was never tested.

The aim of this study is to fill these gaps by characterizing the RBX obtained from Process #2 (hereinafter referred to as RBXP) from a chemical perspective in comparison with two commercial RBXs. To do so, LC-ELSD provided quantitative, carbon number resolved information on the aliphatic composition of the waxes, focusing on the wax esters fraction. FTIR was employed, aiming to identify differences in the minor component fractions. The RBX's structuring ability as oleogelator were compared by forming oleogels with sunflower oil (SO) at different concentrations. Results suggest that a minimum quantity of 1 %wt of RBXP is necessary to obtain a stable oleogel at room temperature. It was also found that a stable crystal network can be formed with RBXP only if the cooling step during oleogel formation is kept at static conditions without any use of stirring. Finally,

thermal and structural analyses confirm that the functional behaviour of the resulting oleogels is strictly related to the nature of the wax used. These findings highlight that the success of the oleogelation process is strictly determined by the purity of the structuring agent. Enhancing wax purity optimizes its oil-binding efficiency and ensures highly reproducible structural properties, a critical requirement for the reliable formulation of lipid-based food products.

# 2. Materials & Methods

## 2.1 Materials

Commercial RBXs were compared with a laboratory-scale isolated RBX obtained according to our previously developed process [38]. The RBX used was recovered from a rice bran butter matrix obtained through supercritical $CO_2$ extraction. Rice bran butter was then subjected to a series of melting, solvent additions, centrifugations, and a final vacuum filtration. The solvent used for all the purification steps was 2-propanol (99.8% pure, Sigma-Aldrich) for its higher efficiency in the RBXP recovery [38]. RBXA was kindly provided by TH.C. TROMM GmbH (Cologne, Germany) and RBXB was kindly provided by KAHL GmbH & Co. KG (Trittau, Germany). Oleogels were formed blending the RBXs with sunflower oil (SO) purchased by a local market (Pam Panorama, Italy). Acetonitrile (ACN), HPLC-grade water ($H_2O$), and HPLC-grade ethanol (EtOH) were purchased from VWR. Methyl-tertiary-butyl-ether (MTBE) and tri-fluoroacetic acid were purchased from Carl Roth. As external standard to compensate for retention time shifts, a mixture of 13 standards of high purity was used, see **Table S1** of Supporting Information.

## 2.2 RBX chemical Characterisation

2.2.1 Liquid ChromatographyNative wax composition was analyzed according to a single-step LC-ELSD method, see Brykczynski et al. 2026 [39]. Standard stock solutions (125 µg/mL per analyte) were prepared in volumetric flasks by adding 99 % (v/v) MTBE and 1 % v/v EtOH to the respective

wax. After dissolution at 35 °C, samples were cooled to ambient temperature, filtered through hydrophobic PTFE filters (0.2 µm pore size), and transferred to injection vials with PTFE septum.

All measurements were performed on an Agilent 1260 Infinity II quaternary system (Agilent Technologies Inc., Waldbronn, Germany) including a G7111B quaternary pump (Agilent, Waldbronn, Germany), G7129C vial sampler with 100 µL injection loop (injection volume 10 µL) (Agilent, Waldbronn, Germany), 1260 Infinity II multicolumn thermostat (Agilent, Waldbronn, Germany) and 1290 II Infinity ELSD (Agilent, Waldbronn, Germany). The nebulizer temperature was 35 °C, the evaporator temperature 90 °C at a nitrogen flow of 1.2 L/min. Nitrogen was produced by a Solaris 10 generator (Peak Scientific Instruments GmbH, Düren, Germany). An OTU MonoKala C18 column without endcapping (105 Å, 5 µm, 250x4.6 mm), protected by a guard column of the same specifications (10x4.6 mm) was employed at 30 °C (both columns: AppliChrom GmbH, Oranienburg, Germany). Two eluents were used at a flowrate of 1 mL/min: Eluent A consists of 99.495 % (v/v) ACN. 0.5 % (v/v) H2O, and 0.005 % (v/v) TFA. Eluent B consists of 98.995 % (v/v) MTBE, 0.5 % (v/v) EtOH and 0.005 % (v/v) TFA. The employed gradient is given in **Table S2** of Supporting Information. Between two runs, a flushing run was performed to ensure cleaning and conditioning of the columns. Measurements were performed in triplicate. Instrument control was performed with the manufacturer's software OpenLab CDS 2.4, data analysis was performed following the workflow of Brykczynski et al. (2026) [39].

2.2.2 Fourier transformation infrared spectroscopy

To record FTIR spectra of the solid wax samples, no further sample preparation was required. Spectra were recorded with a diamond attenuated total reflection (ATR) on a Lyza 7000 FT-IR spectrometer (Anton Paar, Graz, Austria), equipped with an IR source, a KBr-beamsplitter, and a DLaTGS (deuterated L-alanine triglycine sulfate) KBr-detector. All samples were measured in triplicate in the spectral range from 5000 to 500 $cm^{-1}$ using 32 scans at a resolution of 2 $cm^{-1}$. A background spectrum was acquired after every ten measurements. Data processing was carried out using MATLAB

R2021b. For comparability, spectra were shifted to 100% extinction in the region from 4000 to 5000 $cm^{-1}$ and normalised to the band at 2919 $cm^{-1}$.

## 2.3 Oleogelation Process

The oleogelation process was conducted mixing the different RBXs with SO in different proportions. The concentration of RBXP in SO tested were 0.5 %wt, 1 %wt, 2 %wt, 3 %wt, 5%wt, and 10 %wt in a total weight of 1000 mg; RBXA and RBXB were only tested at 1 %wt and 5 %wt concentrations. Samples were prepared in 2 mL vials using the Crystal 16 multi-reactor apparatus (Technobis, Netherlands). With this equipment, 16 samples per time can be prepared, controlling temperature profiles and stirring rates using hook-Hastelloy stirring impellers. The thermal profiles used to form the oleogels and acquire their clear and cloud points data was the one presented in **Table 1.**

**Table 1:** Thermal profiles used for the formation of the oleogels

| Step | Starting Temperature [°C] | Ending Temperature [°C] | Ramp [°C/min] | Holding Time [min] |
|---|---|---|---|---|
| **1** | 20 | 80 | 10 | 10 |
| **2** | 80 | 60 | -10 | 5 |
| **3** | 60 | 20 | -0.5 | 60 |
| **4** | 20 | 80 | 0.3 | 10 |
| **5** | 80 | 70 | -10 | 5 |
| **6** | 70 | 20 | -2 | 60 |

Clear and cloud points were collected using the CrystalClear Software (Technobis, Netherlands). Oleogels referred as "Static" were prepared for all concentration of RBXP by applying a stirring rate of 780 rpm during the steps 1, 2, 4 and 5, and stopping the stirring during the cooling steps 3 and 6. On the other hand, oleogels referred as "Stirred" were prepared only using 1 %wt and 5 %wt RBX concentrations by applying a constant stirring during all the steps of the oleogelation process. These two concentrations were chosen as 1 %wt was determined as the lowest amount of RBXP necessary to form a stable oleogels, and 5 %wt was the highest concentration which guaranteed the least noisy transmissivity in the Crystal 16 apparatus. The stirring rates tested were 300 rpm, 420 rpm, 540 rpm, 660 rpm, 780 rpm, and 900 rpm. These two different conditions were tested to assess how stirring

conditions influence the oleogels formation. Once the oleogels were prepared, they were characterised to examine their thermal, structural, and rheological features.

## 2.4 Stability Assessment and Polarized Light Microscopy Characterisation

After the process in the Crystal 16 equipment ended, the hook impellers were removed and the oleogels were left to settle for a week. To visualize the effect of applying stirring during the oleogel formation phase, pictures of the vials were taken using a Samsung Galaxy A51 (Samsung, South Korea). The microstructural differences for all the different oleogels prepared were analysed through Polarized Light Microscopy (PLM). A bead of oleogel was withdrawn from the vial with a spatula and carefully smeared in the central part of a glass slide then covered with a cover glass. The glass slide was then positioned on a Zeiss Axiolab 5 microscope (Zeiss, Germany) with a polarized light lens. Picture were taken using a 10X magnification lens using again a Samsung Galaxy A51. The post-processing of the images acquired was conducted using ImageJ 1.54d software (USA).

## 2.5 Thermal Characterisation

Differential scanning calorimetry (DSC) was used to highlight the differences in the melting and crystallisation temperatures of the RBXs and their oleogels. A DSC200- Hitachi (Hitachi, Japan) was used to acquire the heat flow measurements. The preparation involved weighing and sealing each sample in an aluminium pan, with an empty pan serving as the reference. For RBX samples a weight of around 4 mg of material was used; for RBX/SO oleogels the quantity used was between 6.5 mg and 8 mg. The RBX samples were heated from 0°C to 100°C with a ramp of 5°C/min and then cooled again to 0°C with a ramp of −2°C/min, for consistency with the measurements conducted in Candela et al., 2025. Since dissolving RBX in SO shifts the phase transition temperatures towards lower temperatures, the heating and cooling for the RBX/SO oleogels were both set between −40°C to 80°C with ramps of ±5°C/min. Experiments were performed under a 50 mL/min nitrogen purge.

## 2.6 Structural Characterisations

### 2.6.1 Synchrotron SAXS/WAXS

Structural insights into RBX and RBX/SO oleogels were obtained through Small Angle / Wide Angle X-ray Scattering (SAXS/WAXS) measurements at the ID02 beamline of the European Synchrotron Radiation Facility (ESRF, France) and at the offline SAXS facility at Diamond Light Source (DLS, UK).

The experimental setup at ESRF featured a commercial Thermo-Haake RS6000 rheometer (Thermo Fisher Scientific, Germany) coupled with a polycarbonate Couette geometry, allowing for simultaneous rheological and structural characterisation. The experimental configuration employed an Eiger2 4M detector (Dectris, DH) for SAXS ($0.45 < q < 58.4$ Å$^{-1}$) and a Rayonix LX 170HS (Rayonix, US) for WAXS ($56.8 < q < 351.7$ Å$^{-1}$), both operating with a beam energy of 12.5 keV ($\lambda$= 1 Å). RBX/SO oleogels prepared with RBXP were melted and a quantity of around 2.5 mL was poured inside the Couette. Samples were brought to 80°C and left at this temperature for around 15 minutes. Then, temperature was cooled at 70°C with a ramp of −1°C/min and kept for 5 minutes. A final ramp to 25°C of -1°C/min concluded the thermal profile. Measurements in shearing conditions were conducted with a constant shear stress ($\gamma$) of 1000 1/s.

At the DLS labSAXS laboratory, SAXS and WAXS data were collected using a Eiger 2 R 1M (SAXS) (75 micron) and a Pilatus 3 R 100K (WAXS) (172 micron) detectors (Dectris), respectively, with an Excillium Ga MetalJet −9.2 keV as electron source. Silver behenate (d-spacing 58.38 Å) and p-bromobenzoic acid served as calibration standards. Samples were loaded into quartz capillaries (1.4 ± 0.1 mm diameter) in their melted state using a 120 mm needle syringe. A Linkam capillary stage CI94 (Linkam Scientific Instrument, UK), The thermal protocol involved an initial cooling down to −5°C, followed by a heating step up to 90°C at 2°C/min. Subsequently, the temperature was ramped down to 25°C at −10°C/min. Data processing was performed using the Peak Analyzer tool in Origin 2018 (OriginLab corporation, USA).

### 2.6.2 Rheological Measurements

The sample with 5 %wt concentration of RBXP in SO was subjected to further rheological assessments. Rheological properties were investigated with an Anton Paar MCR 302 (Anton Paar, Austria) rheometer using a parallel plate setup (25 mm diameter) at a constant gap of 0.5 mm. A bead of the sample to be analysed was spread on the rheometer plate at 25°C and, before starting the measurements, a time period of two minutes was allocated for the sample to reach equilibrium. For the rotational analysis, the shear rate was varied between $10^{-1}$ and $10^{2}$ 1/s. The amplitude sweep tests were conducted with a frequency of 5 Hz, while the frequency sweep tests were conducted with amplitudes of 0.05% and 0.1%.

# 3. Results & Discussion

## 3.1 Chemical Characterisation

### 3.1.1 LC analysis

The aliphatic components of the wax samples were determined by LC-ELSD with a method targeting wax esters, free fatty acids, fatty alcohols and n-alkanes. The chromatograms and the relative mass fractions of the wax ester fraction are shown in **Figure 1**.

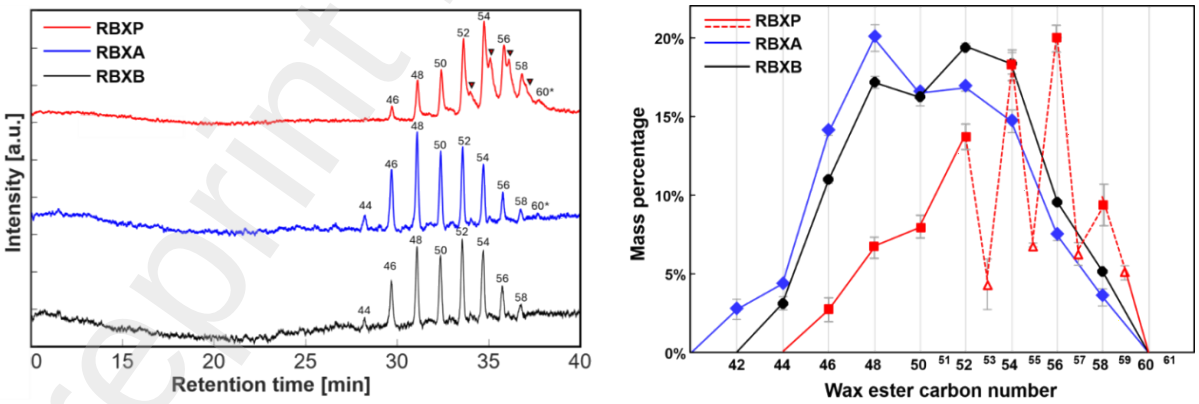


**Figure 1:** LC-ELSD chromatograms and relative mass fractions of the wax ester fraction of the purified and commercial RBXs. *Peak below the limit of quantification

The chromatograms show that all three waxes are mainly composed of long-chained wax esters within a carbon number range from 42 to 60 in the retention time region between 26 and 37 minutes. At lower retention times, only negligible peaks below the limit of quantification have been found. This composition is typical for RBX which is typically reported to contain 95-97 %wt of wax esters[37], [40].

The major differences arising from the wax ester carbon number profiles is the quantitative wax ester distribution. While RBXA (blue) and RBXB (black) exhibit a fairly similar profile with wax esters of carbon number 48 being dominant, the overall carbon number distribution of RBXP (red) is shifted towards higher total carbon numbers. Here, wax esters with a carbon number of 54 are the dominant wax ester. Further, it is clearly visible that RBXP contains significantly higher amounts of odd wax esters than the commercial samples. The overall distribution is narrower for RBXP than for the commercial samples.

Even though the method focuses on the major aliphatic wax constituents, the data allow further conclusions on the composition. During the flushing step of the LC runs, remaining sample which cannot be resolved by the column is washed off. For the commercial samples, a higher intensity at equal concentration was recorded, indicating a higher fraction of non-aliphatic components (see **Figure S1**).

In the results of the previous contribution [38], TAGs were suggested as one possible contamination of RBX samples of lower purity. Dominant TAGs in RBO are composed of palmitic, oleic and linoleic acid [41]. Using the same analytical method, these would elute between 15 and 22 minutes with higher response factors that the other aliphatic components of waxes (data not shown). Therefore, the LC results discourage this hypothesis as this retention time window clearly shows no peaks for none of the waxes.

3.1.2 FTIR analysis

The different RBX samples of different purity have been analysed regarding their functional groups using FTIR spectroscopy. The FTIR spectra of RBXP (red), RBXA (blue) and RBXB (black) are depicted in **Figure 2**. Besides the dominant bands at 2916–2800 $cm^{-1}$ which are typical for the $CH_2$-backbone of hydrocarbon chains [42], all three spectra show characteristic bands for the major components of natural waxes with low variation. At high wave numbers between 3550 and 3100 $cm^{-1}$, exclusively RBXA shows a broad band of low intensity. This is indicative for the presence of –OH stretching vibrations of hydroxyl groups and therefore attributed to free fatty alcohols. All three samples show a clear band at 1734 $cm^{-1}$, with the two commercial samples RBXA and RBXB exhibiting a more pronounced shoulder at 1704 $cm^{-1}$. These bands are caused by the C=O stretching vibrations, which are found in ester bonds (1734 $cm^{-1}$) and carboxyl groups (1704 $cm^{-1}$) [42]. This result is consistent with the wax ester dominated composition of the three waxes as shown by LC analysis and as described in literature[37], [40]. Further, for the commercial samples, smaller fractions of fatty alcohols (RBXA) and fatty acids (RBXB) are indicated. As the LC results did not indicate significant amounts of either component class, this indicates CN number below the detection limit of the LC method (see Brykczynski et al 2026 [39]). For further evidence, comprehensive GC analysis would be required.

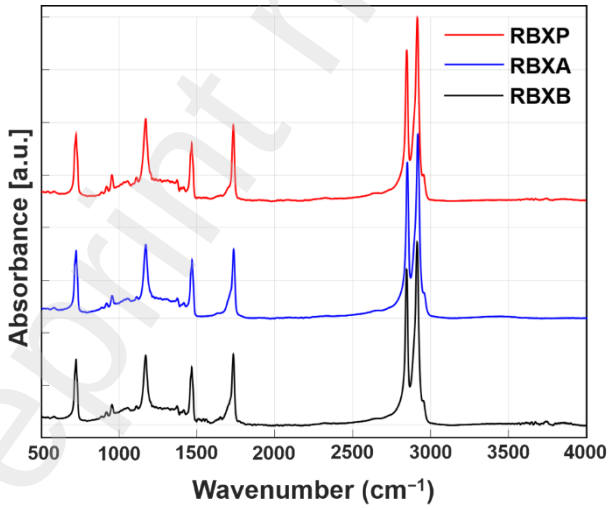


**Figure 2:** FTIR spectra collected for the purified and commercial RBXs samples

No further differences between the three samples were observed, again reflecting the dominance of the wax ester matrix. Consequently, FTIR also provides information on the major chemical constituents of the waxes, while minor components such as phytosterols or γ-oryzanol [41], [43], [44] cannot be resolved reliably due to overlapping absorption bands and their low abundance.

## 3.2 Oleogelation of SO with RBX

SO was used as the oil phase of the oleogels, while RBXP was used as the oleogelator. RBXP was used at various concentrations in the manufacture of oleogels to assess its suitability as a high added-value ingredient. Due to their long-chain ester composition, waxes efficiently structure vegetable oils through high hydrophobicity and low critical gelling concentrations [21], [28]. Moreover, being discarded during oil dewaxing, they represent low-cost alternative to other oleogelators [45].

### 3.2.1 Static Oleogelation

"Static Oleogelation" tests are those not involving agitation during the cooling phase of the oleogelation process. As described in **Section 2.3**, concentrations of 0.5 %wt, 1 %wt, 2 %wt, 3 %wt, 5 %wt and 10 %wt RBXP were used. The minimum oleogelation concentration was considered to be the lowest RBXP quantity at which the oleogel remains firm after its vial has been overturned or shaken. This resulted to be 1 %wt, as also reported in other works [28], [30], [46], [47]. The PLM images shown in **Figure 3** supports this assumption.

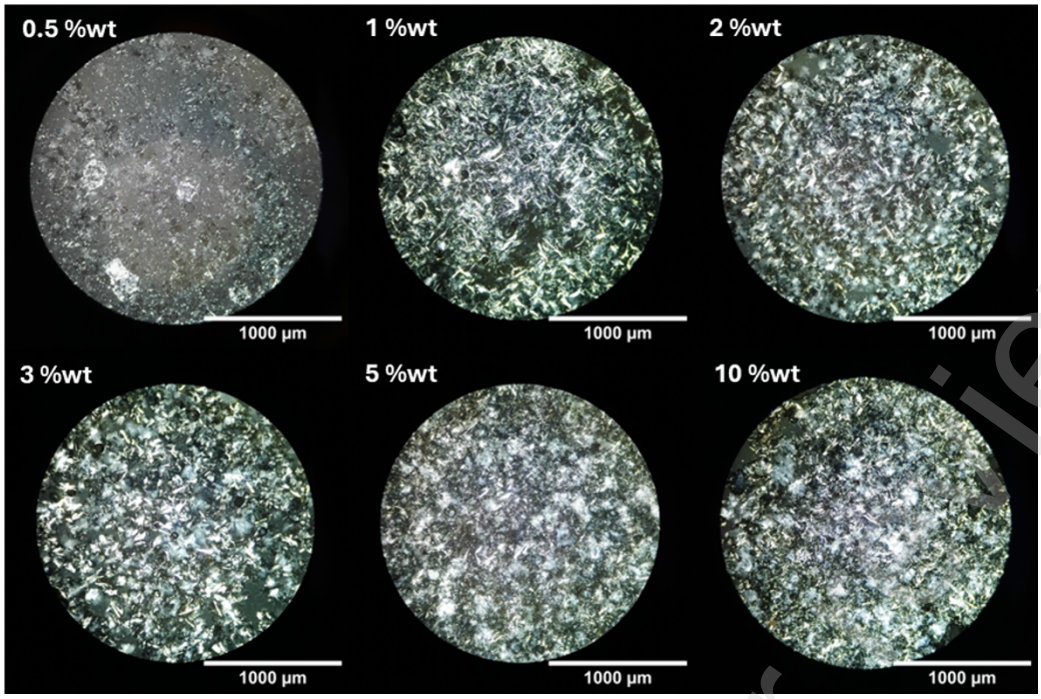


**Figure 3:** PLM images of the RBXP/SO oleogels at Different Concentration formed with static cooling conditions, 10x magnification

316

317 As can be clearly seen, there is a considerable difference between the gel structure obtained at 0.5
318 %wt and 1 %wt. Obviously, this is due to the higher wax content of the 1%wt oleogel compared to
319 the 0.5%wt counterpart. The concentration of RBX also affects the clear temperature ($T_{clear}$) and cloud
320 temperature (hereafter referred to as oleogelation temperature $T_{cloud}$) recorded. These temperatures
321 are summarised in **Table 2**. It is evident that with an increase in RBXP concentration in the
322 formulations, there is a corresponding increase in the relative $T_{clear}$ and $T_{cloud}$, as expected.
323 Macroscopically, no phase separations are observed in oleogels even weeks after preparation (**Figure**
324 **S2** of Supporting Information); this indicates long-term stability at room temperature.

325 **Table 2:** Clear and Cloud temperatures recorded for RBXP/SO oleogels at different RBXP concentrations
326 during static oleogelation process

| Concentration [%wt] | Clear Temperature [°C] | Cloud Temperature [°C] |
|---|---|---|
| 0.5 | 48.5 ± 2.12 | 43.5 ± 0.71 |
| 1 | 54.5 ± 0.71 | 49.7 ± 0.07 |
| 2 | 60.1 ± 0.14 | 55.5 ± 0.07 |
| 3 | 64.2 ± 0.21 | 59.0 ± 0.28 |
| 5 | 66.1 ± 0.35 | 60.0 ± 0.01 |
| 10 | 69.5 ± 0.35 | 64.8 ± 0.35 |

### 3.2.2 Stirred Oleogelation

"Stirred Oleogelation" tests are those involving agitation during the entire oleogelation process. The behaviour of oleogels obtained with agitation was investigated only for samples with a concentration of 1 %wt and 5 %wt of RBXP in SO. Based on the static experiments, these two concentrations were determined to be the most appropriate as 1 %wt was found to be the minimum concentration to obtain stable oleogels, while 5 %wt was determined as the highest tested concentration with low noise level in the transmittivity data acquisition in the Crystal 16 apparatus. The application of stirring appears to affect the network formation of the gels during cooling. As illustrated in **Figure 4**, the compact gel structure that was obtained through the static process (**Figure 3**) is now fragmented and divided into regions of smaller gelled agglomerates. This phenomenon also affects the stability of the oleogels, which begin to exhibit oil separation within few days from their preparation (as can be seen in **Figure S2** of the Supporting Information).

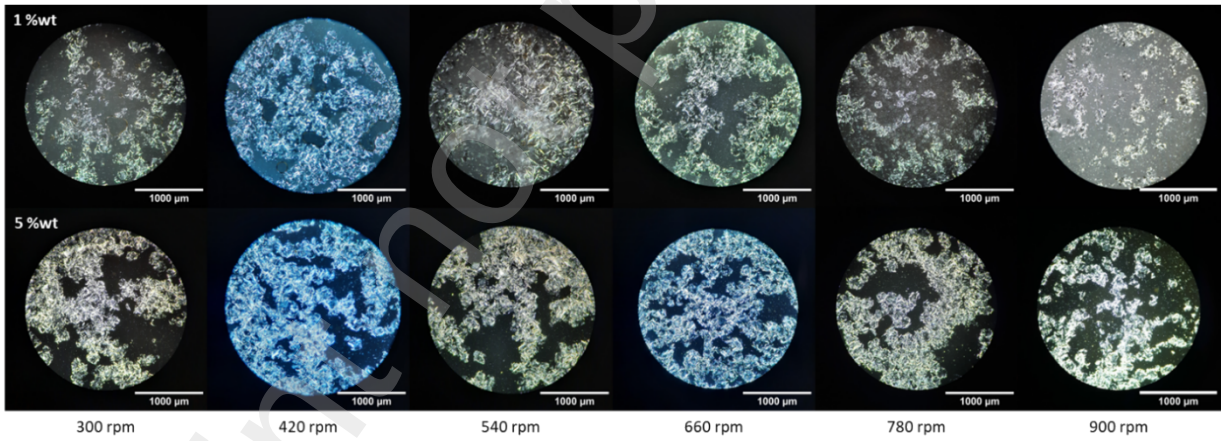


**Figure 4:** PLM images of the 1 %wt and 5 %wt RBXP/SO oleogels at different stirring rates applied, 10x magnification

Furthermore, it is possible to observe how the increase in agitation speed results in the formation of smaller agglomerates. This is evident when the oleogelation is conducted at 900 rpm with the concentration of 1%wt. Subsequently, the recording of the $T_{clear}$ and the $T_{cloud}$ was conducted. The results are summarised in **Table 3** and **Table 4**. Despite the slight deviation observed between the tests at different speeds, it appears that there is no obvious correlation between stirring rate and

recorded clear and cloud points temperatures. In general, it could be observed that the use of agitation during the cooling phase seemed to prevent the formation of a stable oleogel matrix. This behaviour can possibly be attributed both to the obstruction of the sintering due to the stirring effect, and to the fast crystallisation rate of waxes, that hinder the secondary network formation during storage.

**Table 3:** Clear and cloud temperatures recorded for 1 %wt RBXP/SO oleogels at different stirring rates applied during oleogelation

| Stirring Rate [rpm] | Clear Temperature [°C] | Cloud Temperature [°C] |
|---|---|---|
| 0 | 54.5 ± 0.71 | 49.7 ± 0.07 |
| 300 | 55.2 ± 0.50 | 51.8 ± 0.57 |
| 420 | 55.7 ± 0.35 | 52.2 ± 0.07 |
| 540 | 56.4 ± 0.71 | 53.6 ± 0.35 |
| 660 | 56.1 ± 0.78 | 53.6 ± 0.07 |
| 780 | 53.1 ± 1.14 | 52.2 ± 0.61 |
| 900 | 54.0 ± 2.97 | 52.3 ± 1.84 |

**Table 4:** Clear and cloud temperatures recorded for 5 %wt RBXP/SO oleogels at different stirring rates applied during oleogelation

| Stirring Rate [rpm] | Clear Temperature [°C] | Cloud Temperature [°C] |
|---|---|---|
| 0 | 66.1 ± 0.35 | 60.0 ± 0.01 |
| 300 | 65.0 ± 0.14 | 61.5 ± 0.28 |
| 420 | 64.8 ± 0.14 | 61.6 ± 0.21 |
| 540 | 65.7 ± 0.99 | 62.3 ± 1.20 |
| 660 | 65.5 ± 1.06 | 62.5 ± 1.20 |
| 780 | 64.7 ± 0.14 | 60.8 ± 1.11 |
| 900 | 64.7 ± 0.85 | 61.4 ± 1.13 |

3.2.3 Performance evaluation against commercial alternatives

To understand whether the separation during stirring was related to the chemical nature of RBXP, other oleogelation tests were conducted using RBXA and RBXB commercial waxes as oleogelator in SO. Again, 1 % wt and 5 %wt concentrations were taken as reference. At a concentration of 1 %wt, for the oleogels with both commercial waxes in static and stirring conditions, the resulting networks appeared to be not completely formed. Compared to RBXP oleogels, these different formulations

show separation even in static conditions (**Figure 5**). Using a 5 %wt wax content in the same conditions of both RBXA and RBXB, on the other hand, seemed to produce a much more developed microstructure. Under stirring conditions, RBXB formed an oleogel that showed a lower extent of separation and a higher oil-binding efficiency compared to RBXA. This phenomenon might be attributed to some impurities present in this commercial wax, which can stabilize better the three-dimensional network compared to the other waxes tested.

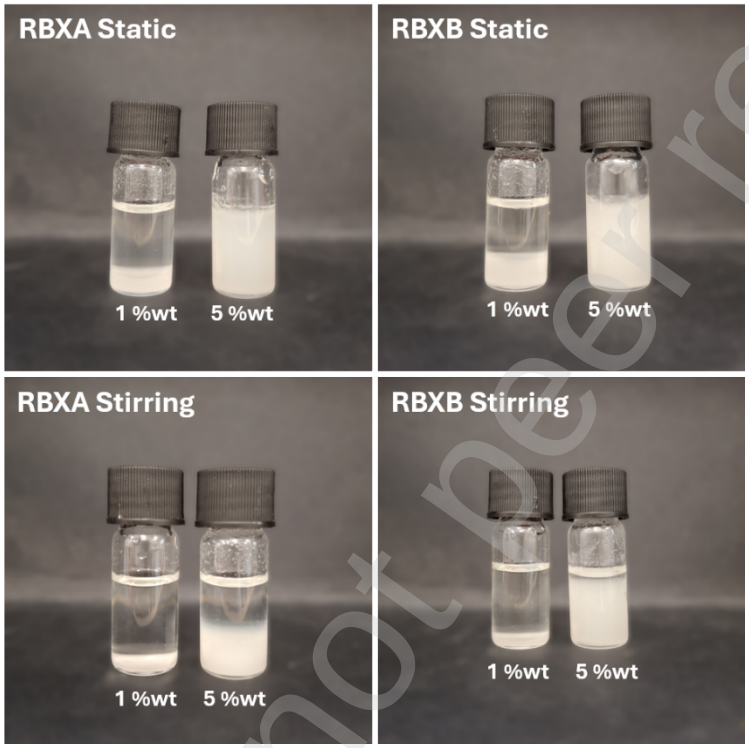


**Figure 5:** Comparison between oleogels obtained with and without stirring in the oleogel formation step using RBXA and RBXB

## 3.3 Thermal Behaviour

To better understand the thermal properties of the oleogels formed with RBXP, RBXA and RBXB, both the RBXs and the RBX/SO oleogels were analysed through DSC. Melting and crystallisation behaviour were recorded more precisely, and a finer comparison was conducted.

### 3.3.1 Starting materials thermal behaviours

**Figure 6** presents the thermogram related to RBXP, RBXA, and RBXB. Furthermore, as a comparison with what previously reported by Candela et al., 2025, another wax (RBX #5) is shown. This choice was made to compare how the different purity (see comparison for chemical characterisation in **Figure S3** of Supporting Information) of the waxes can influence the thermal features recorded during the thermal analysis.

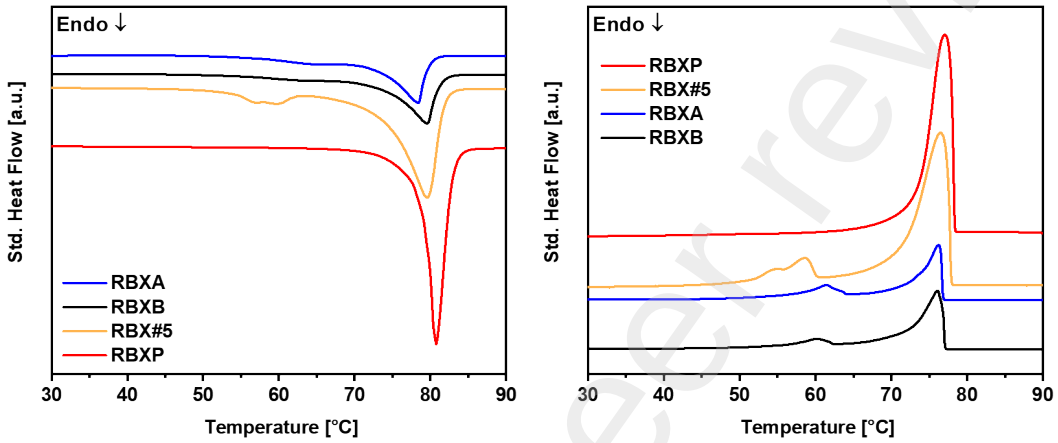


**Figure 6:** Melting and Crystallisation profiles of RBXs tested as oleogelators

Firstly, one should consider the differences between RBXP (red) and RBX #5 (yellow). As already described in the relative paper, varying the purification method may lead to a different chemical composition in the final extract. However, this was not confirmed by the LC analysis, indicating that short-chain fatty acids, fatty alcohols or other minor components in the RBX affect the crystallisation. In the thermogram related to RBX #5 (yellow), two clear peaks between 50°C and 60°C are evident and might be related to these sorts of minor components. The higher purity also influences the narrowness of the peaks related to the wax esters of the extract (above 70°C). Comparing the RBXs obtained by purification with the commercial RBXs, similar considerations can be formulated. Looking at the melting and crystallization profiles, commercial waxes have broader peaks and different melting and crystallisation enthalpies (as shown in **Table 5**). Furthermore, other impurities can be detected when looking at the region below 70°C. In that temperature interval, both RBXA

(blue line) and RBXB (black line) showed a broad and low-intensity peak, a feature becoming more visible when looking at the crystallisation profiles. Having the chemical composition in mind, this might be associated with the minor components presence or with the carbon number profiles within the wax ester fraction. With a broader distribution and almost no odd wax esters, the molecules might form separate crystalline phases. These characteristics are reflected in the relative melting and crystallisation enthalpies, that resulted higher for commercial waxes compared to the purified ones. Overall, the greater stability of RBXP/SO oleogels at 1 %wt content of wax can be justified thanks to its purification extent. In fact, it appeared that RBXP could form a stronger 3D network and hence better entrap the TAGs of SO. On the other hand, this purity extent seems also to have a disadvantageous effect when applying stirring during the oleogelation step. The greater affinity that the wax esters molecules have among each other might lead to the gelled aggregates formation. These aggregates tend to settle at the bottom of the vials leading to the instability of the corresponding oleogels and to oil leakage.

**Table 5:** Melting and Crystallisation Enthalpies comparison of the purified and commercial RBXs

| RBX type | Melting Enthalpy [J/g] | Crystallisation Enthalpy [J/g] |
|---|---|---|
| RBXP | 183.79 | -172.17 |
| RBX#5 | 164.74 | -162.93 |
| RBXA | 193.10 | -183.81 |
| RBXB | 203.88 | -196.43 |

3.3.2 5 %wt Oleogels thermal behaviours

In this subsection, the thermal behaviour of the oleogels formed with RBXP, RBXA, and RBXB in SO is presented. Only data related to the 5 %wt concentration of RBXs are shown since the peaks recorded are more visible with this RBX content. **Figure 7** shows the results related to the DSC analysis conducted on these oleogels.

As it can be expected, the melting and crystallisation profiles of the oleogels formed with RBXP (red) have more defined peaks related to the purity of the wax used. It is clear that, compared to the other oleogels formed with commercial waxes, RBXP/SO oleogel manifests a greater thermal stability. In RBXP/SO oleogel, only one melting and one crystallisation events are recorded. For oleogels prepared with the commercial waxes, instead, one can recognize multiple and broader peaks, possibly related to impurities and their effects on network formation and incorporation of SO.

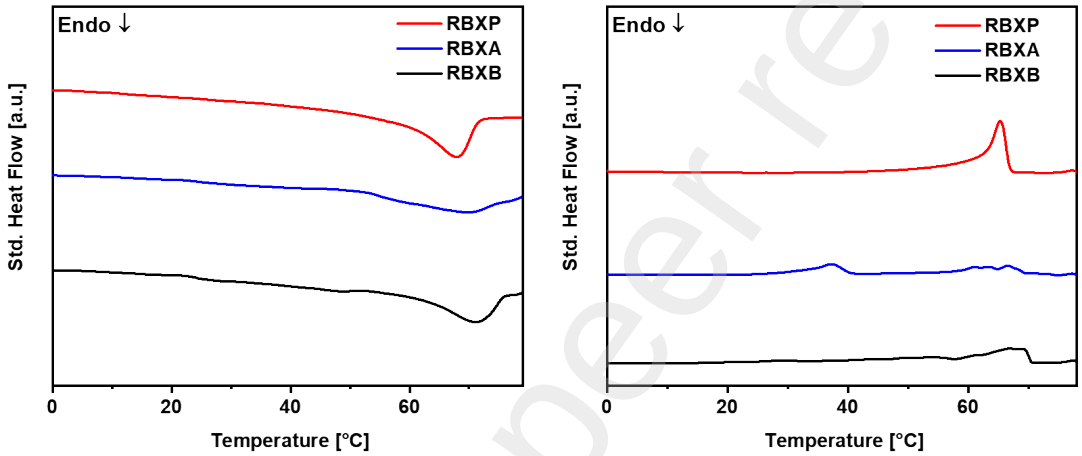


**Figure 7:** Melting and Crystallisation profiles of 5 %wt RBXs/SO

Comparing with the starting RBXP thermal profiles, the oleogel's melting and crystallisation peaks are moved towards lower temperatures due to dissolution of the wax in SO, which is liquid at ambient temperature [27], [28], [35].

## 3.4 Structural Features

### 3.4.1 Rheo-SAXS comparison of RBXP/SO Oleogels

The 1%wt and 5%wt samples were analysed using synchrotron SAXS/WAXS. Tests were conducted at both static and constant shear stress ($\gamma$=1000 $s^{-1}$) conditions provided by the rheometer (see **Section 2.6.1** for further details). **Figure 8** shows the relative diffractograms collected with samples of 5 %wt RBXP in SO.

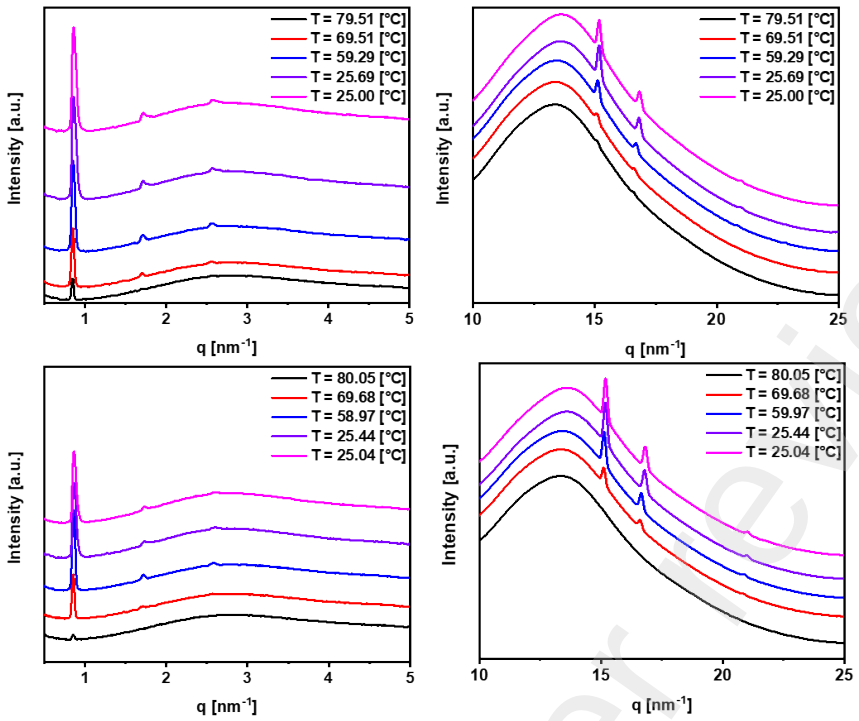


**Figure 8:** SAXS (left side) and WAXS (right side) diffractograms of the 5 %wt RBXP/SO oleogel. Comparison between data recorded without (top part) and with (bottom part) constant shear rate ($\gamma$ = 1000 s-1) applied

A comparison among the graphs of the oleogels with those of the pure wax [38] clearly demonstrates that the blending process with SO has a significant impact on the recorded signal. In the oleogels, a single polymorph is evident in the SAXS region, appearing at around 80°C during cooling. The first peak of this polymorph appears at q = 0.88 $nm^{-1}$ (d-spacing = 7.14 nm) and can be attributed, considering also at the WAXS region, to an orthorhombic perpendicular subcell frequently recorded with waxes obtained from plant-based matrices [48]. Furthermore, by looking at the second and third order reflections, it can be seen a broadening of the peaks, suggesting a possible presence of a segregated crystallisation and overlapping of multiple phases. In the pure RBXP diffractograms, other polymorphs are also observed; however, the blending with SO reduces their signal's intensity and these are not recorded in the oleogels samples. In the WAXS region, the peaks collected are also related to the presence of the orthorhombic perpendicular subcell. A comparison between the oleogels samples obtained with constant shear (applied by the rheometer) and without shear reveals no significant differences in the crystal network formation or polymorphism. This means that the stirring

process does not affect significantly the crystallisation of the fats blend as observed in other systems such as cocoa butter [49], [50], and does not affect the polymorphic behaviour. **Figures S4** shows the same results presented in **Figure 8** but obtained with the 1 %wt RBXP/SO samples. The only differences between these two concentration samples relies on the temperatures of appearing of the crystalline phase: in the 1 %wt sample it appears at 70°C during cooling (around 10°C of difference compared to the 5 %wt sample as also previously showed in the cloud temperatures and DSC data).

SAXS and WAXS profiles were also collected for pure RBXA and RBXB, and for their relative oleogels prepared at the concentration of 5 %wt of wax in SO. Since these samples were not analysed at the same beamline and with a different set up, only capillaries measurements could be collected. The relative data are presented in **Figure S5 - S6**. Both the pure materials only showed a single polymorph with its first peak at around q = 0.87 $nm^{-1}$ and a corresponding d-spacing of 7.22 nm. These values can be attributed to a similar crystallisation pattern as for RBXP an orthorhombic perpendicular subcell. For both waxes the related peaks disappear around 82°C, as also presented during the thermal characterisation section. For the oleogels prepared starting with these two materials, the signal appears noisy (possibly due to the high quantity of oil inside the samples). In any case, one can distinguish again the same polymorph with the first peak in the very same position. In the oleogel RBXA/SO the only visible peak seems to melt at a slightly low temperature compared to RBXB/SO, this behaviour is in agreement with the DSC measurements previously discussed.

Overall, comparing the systems obtained with the recovered refined wax and the commercial counterparts, no significant differences can be recorded or attributed to the nature of the waxes. These findings confirm that samples crystallisation is dominated by the RBXs wax esters, the most present components. Frome the chemical characterisation it was noted that these resulted to be not significantly different. This suggest that the microstructural and functional differences of the oleogels, might be affected by the interactions upon network formation and crystals aggregation, and

474 dominated by other components that was not possible to detect with the analysis performed. All these
475 considerations highlight what can be a critical area for future analytical focus.

476 3.4.2 Rheological characteristics of RBXP/SO Oleogel

477 A first rheological assessment of the oleogels was conducted by recording the viscosity evolution of
478 the samples during the SAXS/WAXS measurements in the Rheo-SAXS environment at ESRF ID02
479 beamline. As it can be noticed in **Figure 9**, the increase of the RBXP concentration induces an
480 increase in the apparent viscosity recorded during the cooling of the samples. This is an expected
481 effect due to the difference of the wax amount in the samples. In this regard, RBXP in higher
482 concentrations immobilises more oil in the 3D structure of the oleogel, leading to an increased
483 resistance to the shear stress applied [35].

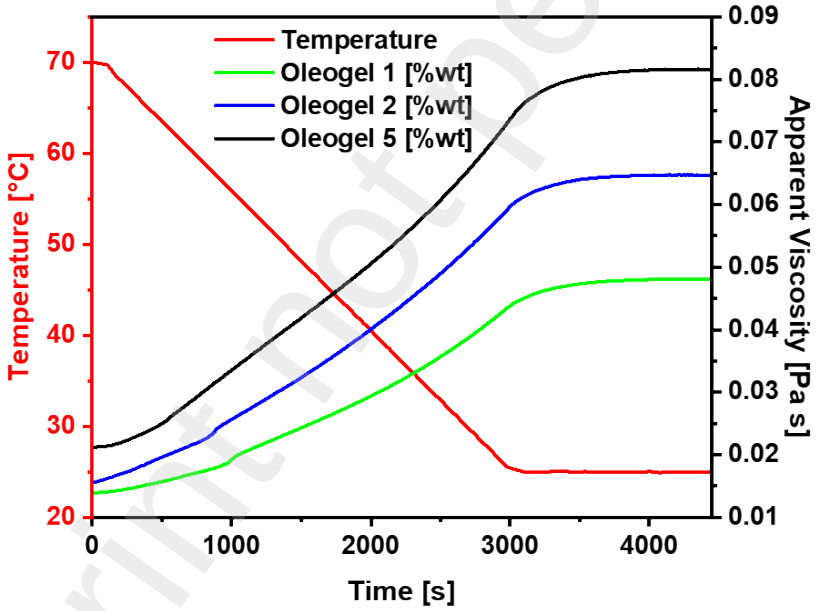


**Figure 9:** Changing of the apparent viscosity of RBXP/SO oleogels during crystallisation. Measurements conducted at constant shear rate ($\gamma = 1000\ s^{-1}$) in the Rheo-SAXS environment of ID02 beamline of ESRF, Grenoble

484

485 To better understand the mechanical features of the RBXP/SO oleogel systems, a complete
486 rheological characterisation was conducted on the 5 %wt sample. This sample was chosen as

benchmark because using a greater amount of wax than 1%wt, resulted in a more accurate data from the instrument.

The amplitude sweep test was utilised to evaluate the oleogel's structural integrity and robustness prior to failure. The test is designed to identify the linear viscoelastic region (LVR), defined as the range of percentage strain within which the oleogel's behaviour can be considered viscoelastic [22]. **Figure 10** shows the results obtained applying a frequency of 5 Hz. The gel-like behaviour is justified by the values of the storage modulus G' and the loss modulus G''. As a matter of fact, in the LVR, the elastic modulus ($G' \approx 2 \cdot 10^4$ Pa) is significantly higher than the viscous modulus ($G'' \approx 7 \cdot 10^3$ Pa). The high absolute value of the modulus G' confirms the effectiveness of the RBXP in forming a robust crystalline network, capable of a distinctly solid and elastic behaviour at rest. However, the recorded LVR appears to be rather short: in fact, both curves begin to drop rapidly before 0.1% strain. This results in a crossover (G' = G'') and, consequently, gel rupture at approximately 0.6% strain. These observations highlight the brittle nature of the developed oleogel structure, which exhibits low elastic resistance before the structural breaking. Similar observations were done by Doan et al., 2015, who found that RBX is able to produce an oleogel with a limited extend of LVR compared to other waxes. The crucial factor highlighted in that work is the affinity between the wax and the oil used, which can determine the strength of the resulting oleogel [22].

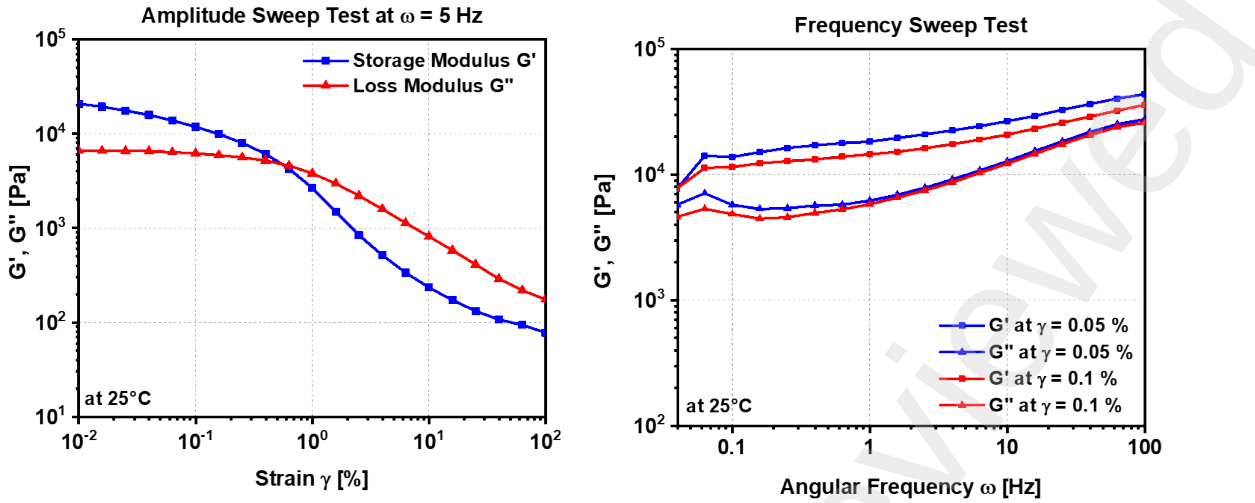


**Figure 10:** Amplitude Sweep test results investigated at 5 Hz fixed frequency (left side); Frequency Sweep test results investigated at 0.05 % and 0.1 % of fixed strain (right side)

The identification of the strain range where oleogel presented a viscoelastic behaviour, allowed the determination of the strain values for the frequency sweep tests (**Figure 10**). These were 0.05 % (before the rapid drop of the moduli in the amplitude sweep test) and 0.1 % (critical value at which both moduli start to drop), both identified inside the LVR. In both cases by varying the frequency in the explored interval, the elastic modulus has always higher values compared to the loss modulus. The same trend was recorded in other works using RBX as oleogelator, where G' was never found to have a crossover point with G'' during frequency sweep tests [22], [35], [51]. These profiles are indicative of a structured system exhibiting a solid-like behaviour, suggesting that the RBXP forms a crystalline framework that can remain stable over time. The solid and elastic behaviours of the oleogels are also justified by the damping factor ($\delta = \tan(G''/G')$) profile by varying the frequency applied (**Figure 11**). In all the points of the explored frequency range, in fact, the value of the damping factor stays below 1, indicating the prevalence of the elastic properties compared to the viscous properties.

Finally, the flow behaviour of the oleogel was evaluated considering complex viscosity and viscosity curves. Measurements were repeated in triplicates and are presented as first, second, and third trial in **Figure 11** and **12**.

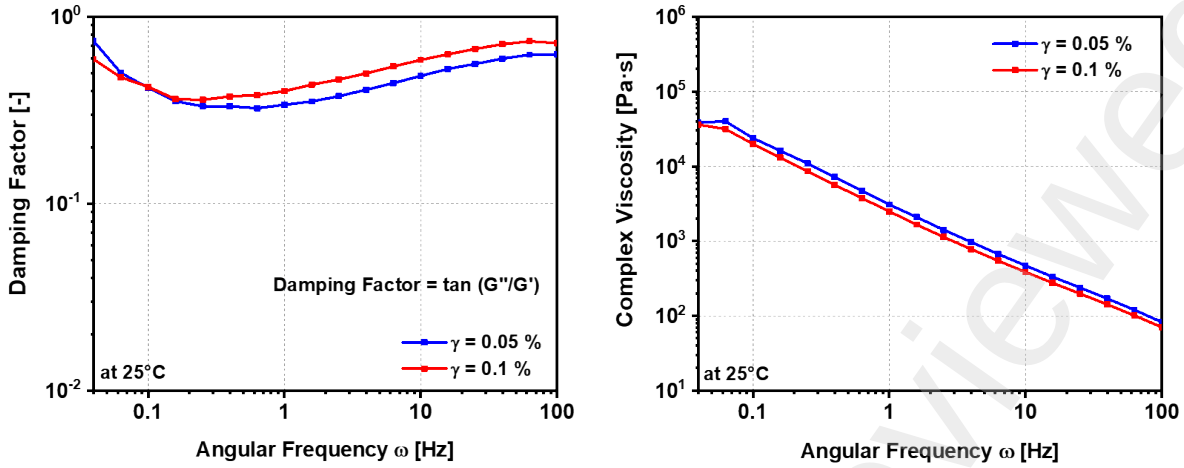


**Figure 11:** Damping Factor (left side) and Complex Viscosity (right side) recorded during the Frequency Sweep oscillatory analysis at 0.05 % and 0.1 % of fixed strain

The analysis were repeated in triplicates and are presented as first, second, and third trial in Both parameters exhibit a marked shear-thinning behaviour, also detected again by Wijarnprecha et al. 2018, and Principato et al. 2021: viscosity decreases by several orders of magnitude as the angular frequency and shear rate increase [35], [51]. However, some fluctuations can be observed in the recorded shear stress profile (**Figure 12** right side): these indicate the presence of some non-uniform fracture of the oleogel or wall slippage during the measurement, confirming the high mechanical fragility of the gel 3D-network previously detected during the amplitude sweep test.

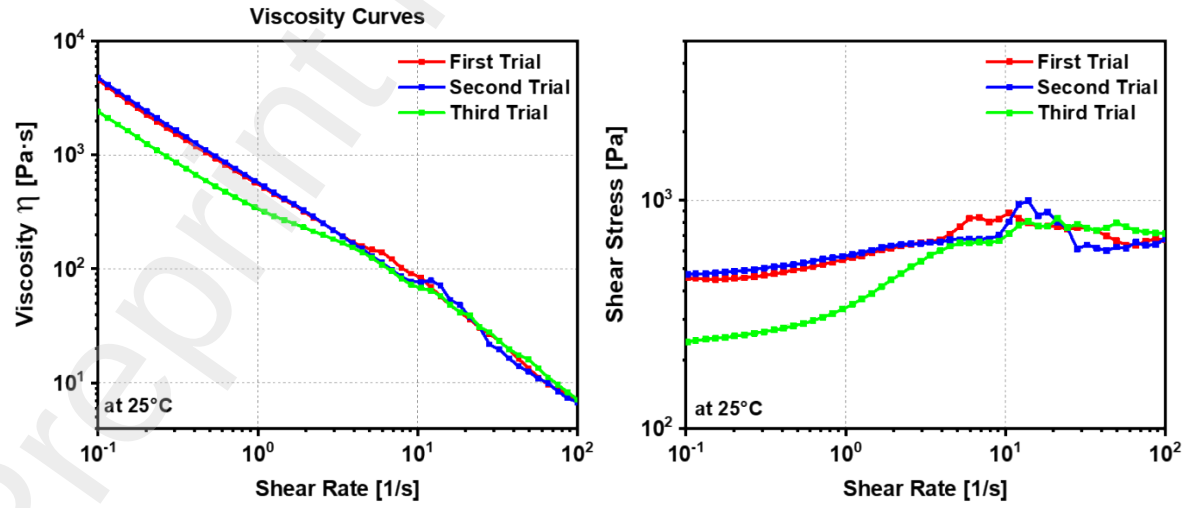


**Figure 12:** Viscosity Curves (left side) and Shear Stress Profiles (right side) recorded during the rotational analysis

## 4. Conclusions

The growing demand for sustainable and healthy ingredients has pushed research toward innovative systems that can provide nutritional benefits without compromising texture and sensory profile. Oleogels are of particular interest due to their ability to create a three-dimensional network by using an oleogelator to structure liquid oils. Among the various structuring agents, RBX has emerged as a promising candidate. However, the functional success of RBX-based oleogels is heavily dependent on the purity of the wax, as residual impurities that can interfere with the formation of the lipid network. Three different RBXs have been used in this study. The specific composition was analysed using LC-ELSD and FTIR, demonstrating the different degrees of purity. While all three waxes were mainly composed of long-chain wax esters, the carbon number profile between the commercial samples and the purified RBX differed substantially with the commercial waxes showing broader distributions lacking in odd wax esters. Minor fractions of free fatty acids and alcohols have been indicated. These compositional differences propagated into the functional properties. The specific composition of the RBX obtained through Process #2, with its high purity and narrow melting range directly influences the microstructural development of the oleogels prepared. The reduced quantity of impurities allows for a more cohesive crystalline network, resulting in enhanced oil-entrapment and stability compared to other RBX commercially available. In particular, within the concentration range investigated under static gelation conditions, the RBX isolated via Process #2 yielded a more stable structure compared to the commercial alternatives (RBXA and RBXB). Furthermore, it was observed that stirring during the oleogelation phase could hinder the development of a solid framework. These conditions, in fact, resulted in the formation of gel aggregates that compromised the oil entrapment, resulting in discreet oil leakage during storage. In conclusion, this research highlights that the development of high-performance oleogels is strictly dependent on both wax purity and the environmental conditions during gelation. The results demonstrate that optimised isolation protocols can transform rice industry by-products into high-value ingredients that can replace existing

commercial alternatives, ensuring uniform properties across products. However, as the analytical methods used to characterize the chemical composition in this publication target the major constituents, alternative methods focusing the minor components might be relevant for further specification. These minor impurities (possibly resulting from sterols, oryzanols and/or glycolipids) seems to not affect the primary crystallisation process but may have a detrimental impact on the network formation and functionality. Moving forward, these findings pave the way for several strategic developments. The stability of the high-purity RBX network suggests a high potential for incorporating these oleogel systems into food matrices, such as bakery products or spreads. Ultimately, this work supports the transition toward a circular bioeconomy, offering a sustainable, clean-label solution for the formulation of lipid-based food products.

## Acknowledgments

This project has received funding from the European Research Council (ERC) under the European Union's Horizon 2020 research and innovation programme (grant agreement No. 949229, CryForm), and the European Union's Horizon Europe research and innovation programme (grant agreement No. 101189244, NewOilFactory). Additionally, it was carried out within the Agritech National Research Center and received funding from the European Union Next-GenerationEU (PIANO NAZIONALE DI RIPRESA E RESILIENZA (PNRR) – MISSIONE 4 COMPONENTE 2, INVESTIMENTO 1.4 – D.D. 1032 17/06/2022, CN00000022). We acknowledge ESRF and Diamond Light Source (DLS) for beamtime on beamlines ID02, and LabSAXS under proposals SC-5464 (ESRF) and SM44335-1 (DLS). We are grateful to beamline scientists Dr Thomas Zinn (DLS), and Dr William Chevremont (ESRF) for the help and support with the two SAXS beamlines and setups used for the work. We would like to thank Mr Michele Lessona, Ms Martina Gaia Baeli and Dr Emmanuele Parisi for their help in collecting data during the beamtimes. A big thanks also goes to Mr Hal Procacci for his help in lab and Mr Francesco Schimmenti for his help with the rheological analyses.

# References


[1] M. Springmann, K. Wiebe, D. Mason-D'croz, T. B. Sulser, M. Rayner, and P. Scarborough, "Health and nutritional aspects of sustainable diet strategies and their association with environmental impacts: a global modelling analysis with country-level detail," 2018. [Online]. Available: www.thelancet.com/

[2] P. Webb *et al.*, "Measurement of diets that are healthy, environmentally sustainable, affordable, and equitable: A scoping review of metrics, findings, and research gaps," 2023, *Frontiers Media S.A.* doi: 10.3389/fnut.2023.1125955.

[3] P. Wang *et al.*, "Optimal dietary patterns for prevention of chronic disease," *Nat. Med.*, vol. 29, no. 3, pp. 719–728, Mar. 2023, doi: 10.1038/s41591-023-02235-5.

[4] S. C. Hull *et al.*, "Diet and Prevention of Cardiovascular Disease and Cancer," Oct. 01, 2025, *Elsevier Inc.* doi: 10.1016/j.jaccao.2025.07.008.

[5] L. Schnabel *et al.*, "Association Between Ultra-Processed Food Consumption and Functional Gastrointestinal Disorders: Results From the French NutriNet-Santé Cohort," *American Journal of Gastroenterology*, vol. 113, no. 8, pp. 1217–1228, Aug. 2018, doi: 10.1038/s41395-018-0137-1.

[6] R. J. De Souza *et al.*, "Intake of saturated and trans unsaturated fatty acids and risk of all cause mortality, cardiovascular disease, and type 2 diabetes: Systematic review and meta-analysis of observational studies," Aug. 12, 2015, *BMJ Publishing Group*. doi: 10.1136/bmj.h3978.

[7] D. Stepanenko, "The Impact of Ultra-Processed Foods on the Risk of Developing Chronic Diseases," *Universal Library of Medical and Health Sciences*, vol. 03, no. 02, pp. 72–78, May 2025, doi: 10.70315/uloap.ulmhs.2025.0302012.

[8] S. Sivakanthan, S. Fawzia, T. Madhujith, and A. Karim, "Synergistic effects of oleogelators in tailoring the properties of oleogels: A review," Jul. 01, 2022, *John Wiley and Sons Inc*. doi: 10.1111/1541-4337.12966.

[9] Z. Wang, J. Chandrapala, T. Truong, and A. Farahnaky, "Oleogels prepared with low molecular weight gelators: Texture, rheology and sensory properties, a review," 2023, *Taylor and Francis Ltd.* doi: 10.1080/10408398.2022.2027339.

[10] C. L. Flores-García, N. Medina-Herrera, B. A. Rodríguez-Romero, G. C. G. Martínez-Ávila, R. Rojas, and Z. Meza-Carranco, "Impact of Fat Replacement by Using Organic-Candelilla-Wax-Based Oleogels on the Physicochemical and Sensorial Properties of a Model Cookie," *Gels*, vol. 9, no. 8, Aug. 2023, doi: 10.3390/gels9080636.

[11] Y. Zhang, J. Xu, C. Tang, and Y. Li, "Crystallization Behavior and Physical Properties of Monoglycerides-Based Oleogels as Function of Oleogelator Concentration," 2023, doi: 10.3390/foods.

[12] M. A. Cerqueira, L. H. Fasolin, C. S. F. Picone, L. M. Pastrana, R. L. Cunha, and A. A. Vicente, "Structural and mechanical properties of organogels: Role of oil and gelator molecular structure," *Food Research International*, vol. 96, pp. 161–170, Jun. 2017, doi: 10.1016/j.foodres.2017.03.021.

[13] M. Kavya, C. Udayarajan, M. J. Fabra, A. López-Rubio, and P. Nisha, "Edible oleogels based on high molecular weight oleogelators and its prospects in food applications," *Crit. Rev. Food Sci. Nutr.*, vol. 64, no. 13, pp. 4432–4455, May 2024, doi: 10.1080/10408398.2022.2142195.

[14] A. J. Martins, F. Cerqueira, A. A. Vicente, R. L. Cunha, L. M. Pastrana, and M. A. Cerqueira, "Gelation Behavior and Stability of Multicomponent Sterol-Based Oleogels," *Gels*, vol. 8, no. 1, Jan. 2022, doi: 10.3390/gels8010037.

[15] T. H. Tan, E. S. Chan, M. Manja, T. K. Tang, E. T. Phuah, and Y. Y. Lee, "Production, health implications and applications of oleogels as fat replacer in food system: A review," Sep. 01, 2023, *John Wiley and Sons Inc*. doi: 10.1002/aocs.12720.

[16] A. A. Abe, I. Aiello, C. Oliviero Rossi, and P. Caputo, "Oleogels: Uses, Applications, and Potential in the Food Industry," Jul. 01, 2025, *Multidisciplinary Digital Publishing Institute (MDPI)*. doi: 10.3390/gels11070563.

[17] D. Thakur, A. Singh, R. Suhag, A. Dhiman, and D. S. Chauhan, "Oleogelation based on plant waxes: characterization and food applications," Dec. 01, 2023, *Springer*. doi: 10.1007/s13197-023-05786-0.

[18] J. Korhonen, A. Honkasalo, and J. Seppälä, "Circular Economy: The Concept and its Limitations," *Ecological Economics*, vol. 143, pp. 37–46, Jan. 2018, doi: 10.1016/J.ECOLECON.2017.06.041.

[19] B. Esposito, M. R. Sessa, D. Sica, and O. Malandrino, "Towards circular economy in the agri-food sector. A systematic literature review," Sep. 01, 2020, *MDPI*. doi: 10.3390/SU12187401.

[20] C. D. Doan *et al.*, "Crystallization and Gelation Behavior of Low- and High Melting Waxes in Rice Bran Oil: a Case-Study on Berry Wax and Sunflower Wax," *Food Biophys.*, vol. 12, no. 1, pp. 97–108, Mar. 2017, doi: 10.1007/s11483-016-9467-y.

[21] D. Dimakopoulou-Papazoglou, K. Zampouni, and E. Katsanidis, "Natural Waxes as Gelators in Edible Structured Oil Systems: A Review," Aug. 01, 2025, *Multidisciplinary Digital Publishing Institute (MDPI)*. doi: 10.3390/gels11080656.

[22] C. D. Doan, D. Van De Walle, K. Dewettinck, and A. R. Patel, "Evaluating the oil-gelling properties of natural waxes in rice bran oil: Rheological, thermal, and microstructural study," *JAOCS, Journal of the American Oil Chemists' Society*, vol. 92, no. 6, pp. 801–811, Jun. 2015, doi: 10.1007/s11746-015-2645-0.

[23] M. Loiacono, L. Padovano, M. C. Malacarne, S. Conti, and E. Caruso, "Formulation and evaluation of alternative to beeswax for vegan lipsticks," *Int. J. Cosmet. Sci.*, vol. 47, no. 4, pp. 626–638, Aug. 2025, doi: https://doi.org/10.1111/ics.13060.

[24] I. Tavernier, C. D. Doan, D. Van De Walle, S. Danthine, T. Rimaux, and K. Dewettinck, "Sequential crystallization of high and low melting waxes to improve oil structuring in wax-based oleogels," *RSC Adv.*, vol. 7, no. 20, pp. 12113–12125, 2017, doi: 10.1039/c6ra27650d.

[25] J. L. Hargrove, P. Greenspan, and D. K. Hartlet, "Nutritional Significance and Metabolism of Very Long Chain Fatty Alcohols and Acids from Dietary Waxes," 2004.

[26] Y. Athukorala, G. Mazza, and B. Dave Oomah, "Extraction, purification and characterization of wax from flax (Linum usitatissimum) straw," *European Journal of Lipid Science and Technology*, vol. 111, no. 7, pp. 705–714, Jul. 2009, doi: 10.1002/ejlt.200800269.

[27] S. A. Holey, K. P. C. Sekhar, S. S. Mishra, S. Kanjilal, and R. R. Nayak, "Effect of oil unsaturation and wax composition on stability, properties and food applicability of oleogels," *J. Am. Oil Chem. Soc.*, vol. 98, no. 12, pp. 1189–1203, Dec. 2021, doi: https://doi.org/10.1002/aocs.12536.

[28] A. I. Blake, E. D. Co, and A. G. Marangoni, "Structure and Physical Properties of Plant Wax Crystal Networks and Their Relationship to Oil Binding Capacity," *J. Am. Oil Chem. Soc.*, vol. 91, no. 6, pp. 885–903, Jun. 2014, doi: https://doi.org/10.1007/s11746-014-2435-0.

[29] Y. Shi, C. Liu, Z. Zheng, X. Chai, W. Han, and Y. Liu, "Gelation behavior and crystal network of natural waxes and corresponding binary blends in high-oleic sunflower oil," *J. Food Sci.*, vol. 86, no. 9, pp. 3987–4000, Sep. 2021, doi: 10.1111/1750-3841.15840.

[30] L. S. K. Dassanayake, D. R. Kodali, S. Ueno, and K. Sato, “Physical properties of rice bran wax in bulk and organogels,” *JAOCS, Journal of the American Oil Chemists’ Society*, vol. 86, no. 12, pp. 1163–1173, Jan. 2009, doi: 10.1007/s11746-009-1464-6.

[31] N. Wang *et al.*, “Crude Wax Extracted from Rice Bran Oil Improves Oleogel Properties and Oxidative Stability,” *European Journal of Lipid Science and Technology*, vol. 123, no. 6, Jun. 2021, doi: 10.1002/ejlt.202000091.

[32] H. M. Bayomy and S. E. Almasoudi, “Physicochemical properties of oleogels based on sunflower or soybean oil structured with rice bran wax,” *LWT*, vol. 238, Dec. 2025, doi: 10.1016/j.lwt.2025.118845.

[33] S. Sahu, M. Ghosh, and D. K. Bhattacharyya, “Utilization of unsaponifiable matter from rice bran oil fatty acid distillate for preparing an antioxidant-rich oleogel and evaluation of its properties,” *Grasas y Aceites*, vol. 71, no. 1, 2020, doi: 10.3989/gya.0938182.

[34] L. S. K. Dassanayake, D. R. Kodali, and S. Ueno, “Formation of oleogels based on edible lipid materials,” Oct. 2011. doi: 10.1016/j.cocis.2011.05.005.

[35] K. Wijarnprecha, K. Aryusuk, P. Santiwattana, S. Sonwai, and D. Rousseau, “Structure and rheology of oleogels made from rice bran wax and rice bran oil,” *Food Research International*, vol. 112, pp. 199–208, Oct. 2018, doi: 10.1016/j.foodres.2018.06.005.

[36] T. Wettlaufer, H. Brykczynski, and E. Flöter, “Wax-Based Oleogels—Properties in Medium Chain Triglycerides and Canola Oil,” *European Journal of Lipid Science and Technology*, vol. 124, no. 2, Feb. 2021, doi: 10.1002/ejlt.202100114.

[37] C. D. Doan *et al.*, “Chemical profiling of the major components in natural waxes to elucidate their role in liquid oil structuring,” *Food Chem.*, vol. 214, pp. 717–725, Jan. 2017, doi: 10.1016/J.FOODCHEM.2016.07.123.

[38] D. Candela *et al.*, “Valorization of the lipid fraction of rice bran via supercritical CO2 and green solvent extraction processes,” *Applied Food Research*, vol. 5, no. 2, Dec. 2025, doi: 10.1016/j.afres.2025.101285.

[39] H. Brykczynski, E. S. J. Rudolph-Flöter, V. Schreiber, and E. Flöter, “A novel, single-step LC-ELSD method to characterize the aliphatic fraction of natural waxes,” *Food Chem.*, vol. 510, May 2026, doi: 10.1016/j.foodchem.2026.148570.

[40] S. R. Vali, Y. Ju, T. N. B. Kaimal, and Y. Chern, “A process for the preparation of food-grade rice bran wax and the determination of its composition,” *J. Am. Oil Chem. Soc.*, vol. 82, no. 1, pp. 57–64, Jan. 2005, doi: 10.1007/s11746-005-1043-z.

[41] T. MIYAZAWA, H. TAZAWA, and Y. FUJINO, “MOLECULAR SPECIES OF TRIGLYCERIDE IN RICE BRAN,” *Cereal Chem.*, vol. 2, pp. 138–145, 1978.

[42] G. Socrates, “Infrared and Raman characteristic group frequencies : tables and charts,” 2010. [Online]. Available: https://api.semanticscholar.org/CorpusID:92333066

[43] A. G. Gopala Krishna, K. H. Hemakumar, and S. Khatoon, “Study on the composition of rice bran oil and its higher free fatty acids value,” *JAOCS, Journal of the American Oil Chemists’ Society*, vol. 83, no. 2, pp. 117–120, Feb. 2006, doi: 10.1007/s11746-006-1183-1.

[44] Champagne Elaine T., Ed., *Rice : chemistry and technology*. American Association of Cereal Chemists, 2004.

[45] C. D. Doan, I. Tavernier, P. K. Okuro, and K. Dewettinck, "Internal and external factors affecting the crystallization, gelation and applicability of wax-based oleogels in food industry," Feb. 01, 2018, *Elsevier Ltd*. doi: 10.1016/j.ifset.2017.09.023.

[46] L. Samuditha, K. Dassanayake, D. R. Kodali, S. Ueno, and K. Sato, "Crystallization Kinetics of Organogels Prepared by Rice Bran Wax and Vegetable Oils," 2012. [Online]. Available: http://www.jstage.jst.go.jp/browse/jos/http://mc.manusriptcentral.com/jjocs

[47] J. F. Toro-Vazquez, J. A. Morales-Rueda, E. Dibildox-Alvarado, M. Charó-Alonso, M. Alonzo-Macias, and M. M. González-Chávez, "Thermal and textural properties of organogels developed by candelilla wax in safflower oil," *JAOCS, Journal of the American Oil Chemists' Society*, vol. 84, no. 11, pp. 989–1000, Nov. 2007, doi: 10.1007/s11746-007-1139-0.

[48] S. Pandolsook and S. Kupongsak, "Potential use of policosanol extract from Thai bleached rice bran wax as an organogelator," *Journal of Food Measurement and Characterization*, vol. 14, no. 4, pp. 2078–2086, Aug. 2020, doi: 10.1007/s11694-020-00455-8.

[49] E. M. Castro-Alayo, C. R. Balcázar-Zumaeta, L. Torrejón-Valqui, M. Medina-Mendoza, I. S. Cayo-Colca, and F. P. Cárdenas-Toro, "Effect of tempering and cocoa butter equivalents on crystallization kinetics, polymorphism, melting, and physical properties of dark chocolates," *LWT*, vol. 173, Jan. 2023, doi: 10.1016/j.lwt.2022.114402.

[50] J. Chen, S. M. Ghazani, J. A. Stobbs, and A. G. Marangoni, "Tempering of cocoa butter and chocolate using minor lipidic components," *Nat. Commun.*, vol. 12, no. 1, Dec. 2021, doi: 10.1038/s41467-021-25206-1.

[51] L. Principato *et al.*, "Effect of dietary fiber and thermal conditions on rice bran wax-based structured edible oils," *Foods*, vol. 10, no. 12, Dec. 2021, doi: 10.3390/foods10123072.